Crystallographic Characterization of an Electroplated Zinc Coating Prone to Whiskers

Auriane Etienne, Emmanuel Cadel, Agnès Lina, Laurent Cretinon, Philippe Pareige

Crystallographic Characterization of an Electroplated Zinc Coating Prone to Whiskers

Auriane Etienne, Emmanuel Cadel, Agnès Lina, Laurent Cretinon, and Philippe Pareige

***Abstract*— A Zn-electroplated steel prone to Zn whiskers has been investigated in order to obtain information about the microstructure of the Zn coating at the root of a whisker. Indeed, the characterization of the Zn coating is essential to understand the Zn whisker growth mechanism. Care was taken to prepare a sample at a whisker root by using a focused-ion beam in a dual-beam scanning electron microscope. The sample was analyzed using energy dispersive X-ray spectrometry and electron backscattered diffraction. Results show three different regions: 1) an inclusion enriched with Ca, Al, and C; 2) the Zn coating with columnar grains; and 3) the root of the whisker. An important point is that recrystallized grains are found at the whisker root. This observation supports recent whisker growth models based on recrystallization.**

***Index Terms*— Electron scattering diffraction, electroplating, focused-ion beam, recrystallization, Zn whiskers.**

I. Introduction

METALLIC whiskering has been under high consideration in the electronic industry since the 1940s, when it was found that cadmium whiskers cause short circuits of electrical hardware [1]. Whiskers grow spontaneously from electroplates like cadmium, zinc, or tin coatings at room temperature. Metallic whiskers show different morphologies: 1) whisker needles whose length can reach several millimeters [2]; 2) kinked whiskers that have sudden change in growth direction; and 3) whiskers in the form of nodules from which needles can grow. Although whiskers have been studied for several decades, the mechanism of whisker growth is still not well understood.

While a large number of studies [2]–[7] have been focused on tin whiskers and minimization of their growth, only a limited number of researches were interested on zinc whiskers [8]–[11].

Electroplated zinc coatings are usually used as anticorrosive layer for low alloy steels. These Zn-coated steels are used for electronic components in automotive, aerospatial, or energy industry, but also for support structures or raised-floor tiles in computer data centers [8], [10]. The risk of electrical or electronic disturbances caused by Zn whiskers is significant, as shown, for example, by a NASA data center report [8]. In order to avoid these disturbances, whisker growth needs to be mitigated and so, mechanisms of whisker growth need to be clarified.

The first step toward the understanding of whisker growth mechanism is a micro- or nano-structural characterization of Zn whiskers and their coatings. In this paper, an electroplated Zn coating prone to whiskers has been investigated using dual beam scanning electron microscope/focused ion beam (SEM/FIB), electron backscattered diffraction (EBSD) and X-ray energy-dispersive spectroscopy (EDS). The originality of this paper lies on the fact that samples for EBSD and EDS were prepared at the root of the whisker using SEM/FIB.

II. Experiments

The studied material is a low alloy carbon steel, namely S235, coated with a Zn electroplating. A final chromate conversion coating of about 200 nm in thickness was applied to the material. The thickness of the Zn coating is about 10 μm on a 620-μm steel substrate. The material was fabricated in 1982. The details of the electroplating process are not known. The specimen investigated was used for several decades as an armour plate in an electronic device.

The residual stress and texture of the electroplated surface were measured by X-ray diffraction (XRD) using a Goniometer Siemens D500.

Samples for EBSD and EDS were removed from the material using the lift-out technique in a Zeiss Nvision 40 SMT dual beam SEM/FIB following this procedure.

1) A protective platinum cap of 0.1 μm in thickness is deposited over the region of interest (the root of the whisker).
2) A Ga ion beam milled section of the region is fabricated by a lift-out procedure. First, at a coupon tilted 0° with respect to the ion beam direction, a trapeze about 8 μm wide and $\approx$20 μm length is milled. A second trapeze is then milled over the other side of the protective cap to obtain a slice. The bottom and one side of the

This work was supported in part by the framework of the Carnot Institute Energy and Propulsion Systems and in collaboration with the EDF R&D Research Centre of Les Renardières. Recommended for publication by Associate Editor G. Galyon upon evaluation of reviewers' comments.

A. Etienne, E. Cadel, and P. Pareige are with the Groupe de Physique des Matériaux, Université et INSA de Rouen, UMR CNRS 6634, Saint Etienne du Rouvray Cedex 76801, France (e-mail: auriane.etienne@gmail.com; emmanuel.cadel@univ-rouen.fr; philippe.pareige@univ-rouen.fr).

A. Lina is with the Department of Materials and Mechanics of Components, Corrosion Studies Laboratory, EDF R&D, Moret sur Loing Cedex 77818, France (e-mail: agnes.lina@edf.fr).

L. Cretinon is with the Electrical Equipment Laboratory, EDF R&D, Moret sur Loing Cedex 77818, France, and also with EDF SEPTEN, Villeurbanne Cedex 69628, France (e-mail: laurent.cretinon@edf.fr).

Digital Object Identifier 10.1109/TCPMT.2012.2203134

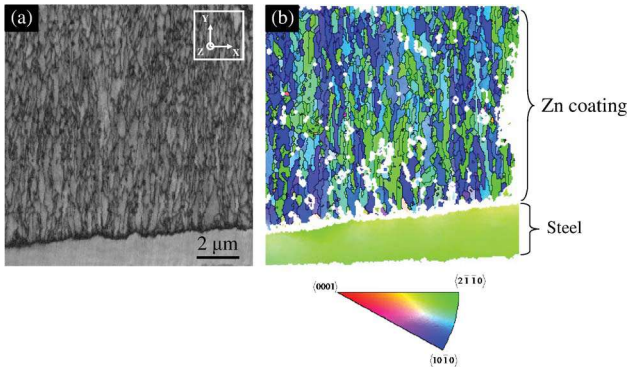

Fig. 1. (a) Band contrast image obtained by EBSD on a sample extracted from the coating far from a whisker. The grain structure is clearly visible. The steel substrate is visible at the bottom of the image. (b) EBSD inverse pole figure of the Zn coating with respect to the y-axis direction obtained on the sample extracted from the coating far from a whisker. The grain structure (grain boundary angle higher than 10°) is highlighted with black lines in the Zn coating.

slice are then cut free. The lift-out slice is attached with a platinum deposit to a micromanipulator probe. The second side of the lift out is then cut free, resulting in a $\sim 15 \times 12 \times 2$ μm^3 rectangular cuboid shaped specimen blank.

3) The sample is then attached by one side to a Cu grid using a platinum deposition.
4) One face of the rough blank is then polished with Ga ions. The final milling was performed at Ga beam energy of 30 keV at a current of about 80 pA.

The EBSD experiments were carried out in the same dual beam SEM/FIB using a 20 keV electron beam with a current of 1.5 nA. The EBSD step size was 50 nm. EBSD patterns were acquired and indexed using an HKL Nordlys II detector and Channel 5 software (Oxford Instruments). A pixel binning of 2×2 was applied for pattern acquisition. At the beginning of the data treatment, a noise reduction was applied. First, wild spikes (isolated points that have been incorrectly indexed) are extrapolated using copies of all neighboring points. Then, a zero solution (diffraction patterns that could not be indexed) extrapolation is applied using six of the neighboring points.

The EDS experiments were performed in a Zeiss 1530 SEM operated at 20 keV using an Oxford Instruments INCA EDS equipment.

III. Results

The Zn-electroplated coating studied shows some needle-like whiskers arising from nodules. It should be noted that some whiskers do not have nodule and some nodules do not give rise to needle-like whiskers. Between 30 and 40 nodules or whiskers were observed per mm^2 area. The diameter of whiskers varies between 1.5 and 4 μm. The length of whiskers is up to 8 mm.

XRD measurements of the residual stress by the $\sin^2\Psi$ method indicate that the coating is, after 27 years of service, under a compressive stress of approximately (30 ± 9) MPa. The compressive stress is a little lower than the one measured on a new Zn coating (compressive stress between 51 and 71 MPa) from a previous study [12]. This indicates that a small stress relaxation has occurred. These values are in the same order of magnitude than the internal stress measured by [9] on a series of Zn-electroplated samples elaborated in different plating baths.

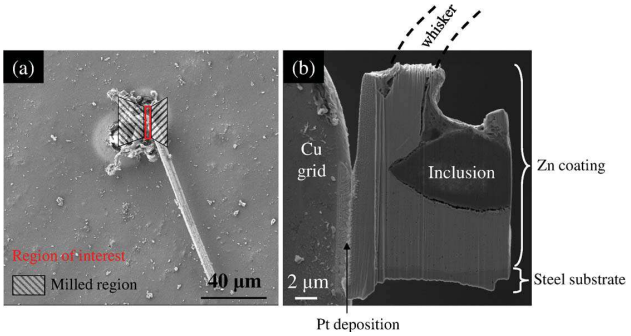

Fig. 2. (a) SEM top view of the milled blank removed from the root of the whisker. (b) SEM side view of the milled blank glued on the Cu grid and polished with Ga ions.

The presence of a texture in the coating can also be determined using XRD measurements. A fibber texture is present in the coating with $\{11\bar{2}0\}$ planes parallel to the surface. The same preferred crystallographic orientation was shown in Zn coatings by [9].

One sample was extracted from the Zn coating far from a whisker. The EBSD band contrast (BC) image and the EBSD inverse pole figure image with respect to the y-axis direction are depicted in Fig. 1(a) and (b), respectively. The grain structure of the Zn coating is clearly visible. The Zn coating is composed by columnar grains of 1.5 μm long and 0.3 μm wide. The texture obtained by EBSD is consistent with the one obtained by XRD that is to say planes between $\{\bar{1}2\bar{1}0\}$ (planes perpendicular to the $<2\bar{1}\bar{1}0>$ direction, in blue) and $\{10\bar{1}0\}$ (planes perpendicular to the $<10\bar{1}0>$ direction, in green) are parallel to the surface.

A second sample was extracted at the root of a whisker and was analyzed by EDS and EBSD. The sample under the whisker was removed from the coating under a whisker as it is shown in Fig. 2(a). Care was taken to be sure that it was prepared at the whisker root. The root of the whisker is indicated with dotted lines in Fig. 2(b).

First of all, an inclusion of approximately 10 μm large is clearly visible as depicted on the SEM side view of the sample [Fig. 2(b)]. EDS measurements indicate that this inclusion is enriched with C, Al, and Ca. Average atomic concentrations are, respectively, ∼50%, ∼30%, and ∼15%. Only some traces of Fe and Zn are detected. Some amounts of Mg and Ga are also detected (respectively, 0.8% and 0.7%). Ga is probably coming from the ion polishing. The origin of this inclusion is not easy to determine. One of the hypotheses could be that the impurities are coming from the electroplating bath. According to previous analysis by high resolution glow discharge mass spectrometry performed by EDF [12], about 1500 ppm of Na are present in the Zn coating. This could indicate, with the relative age of the sample, that a basic cyanide bath was used for the electroplating. In this kind of baths, several chemicals could be added [13], for example: 1) calcium sulfate or hydrate to avoid the formation of carbonate and

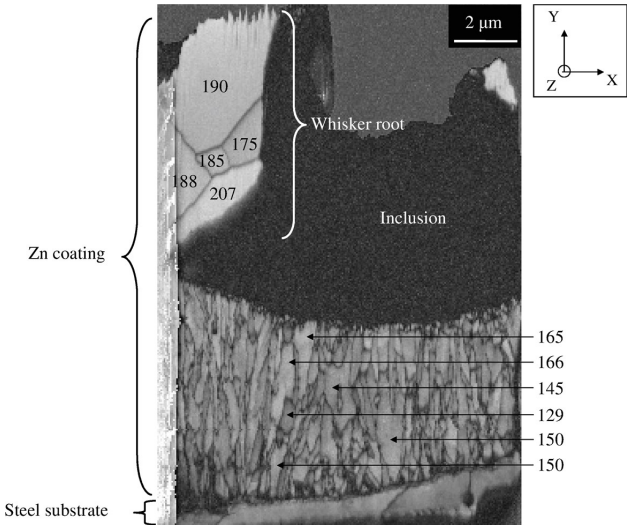

Fig. 3. EBSD pattern quality map depicting the grain structure of the Zn coating on the sample extracted at the root of a whisker. The steel substrate is visible at the bottom of the sample. No diffraction pattern was obtained from the inclusion. Two regions can be distinguished in the Zn coating, one composed of columnar grain with vertical grain boundaries and one composed by larger grains at the root of the whisker with oblique grain boundaries. Some quality factors are reported for these two regions. The three axes of the sample orientation are given in the top right of the figure.

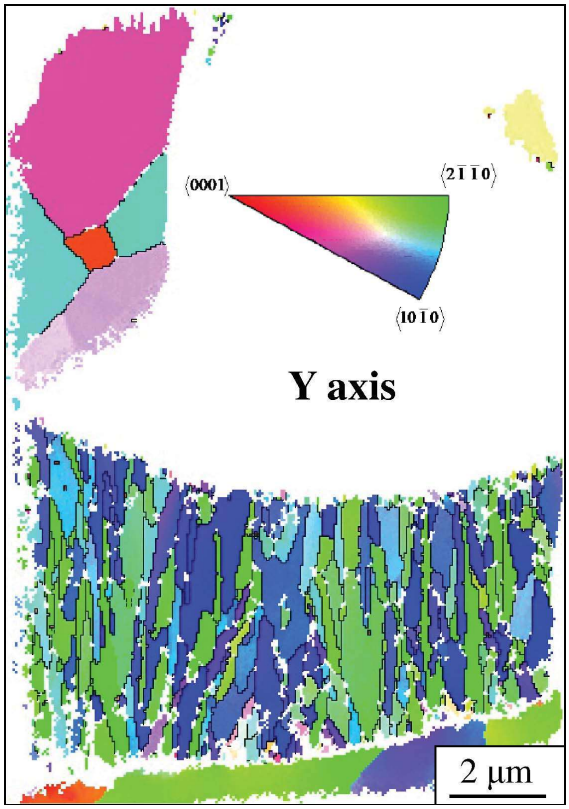

Fig. 4. EBSD inverse pole figure of the Zn coating with respect to the y-axis direction on the sample extracted at the root of a whisker. The grain structure (grain boundary angle higher than 10°) is highlighted with black lines in the Zn coating.

2) aluminum sulfate to improve the quality of the coating. In addition, anodes used for basic baths are sometimes made of Ca–Zn, Mg–Zn, or Al–Zn alloys [13]. So some Ca or Al impurities could be trapped in the Zn coating during the electrodeposition. Equally, impurities could have settled during water rinsing after the electrodeposition as it has been already observed in [14].

No diffraction signal was obtained from the inclusion region as it can be seen in Fig. 3. This suggests that the inclusion is not crystalline but amorphous. Further investigations are needed to determine if the presence of inclusions has a role on the formation of whiskers.

In Fig. 3 is depicted the BC image, which is correlated with the diffraction pattern quality factor [15]. The quality factor is usually related to topography variations and phase differences. In our case, except the presence of the inclusion, the coating is only Zn and there is no topography variation due to the FIB preparation. Diffraction patterns along grain boundaries generally show poor quality factor (black on the BC image). On the contrary, diffraction patterns quality in nondeformed regions of a grain is high (white on the BC image). So, the BC image not only brings information about the grain structure but also about the density of defects and/or recrystallization. In Fig. 3, the grain structure into the Zn coating is clearly visible. First of all, two different regions into the Zn coating can be distinguished: 1) one composed of columnar grain of about 270 nm wide and approximately 1.50 μm long with vertical grain boundaries (called columnar region in the following), the grain structure in this region is similar to the one in the coating far from whiskers and 2) one composed by larger grains at the root of the whisker with oblique grain boundaries (called root region in the following). These two regions are made of the same phase, i.e., pure Zn. Although both are located in the Zn coating, a difference of BC is observed as it is shown in Fig. 3. The average quality factor is approximately 190 in the root region and 150 in the columnar region. This difference is explained by a difference in defect and/or dislocation density in grains between both regions. This observation, combined with the fact that grains are larger in the root region than in the columnar region, suggests that grains at the root of the whisker are recrystallized.

The quality factor difference, visible on the BC image, between the root region and the columnar region, needs to be interpreted with care. Indeed, BC image interpretation could be difficult because BC can also be affected, in some cases, by the phase, the surface tilt, and the orientation [16], [17]. The inverse pole figure images with respect to the y-axis direction is depicted in Fig. 4. It clearly appears that, in the columnar region, planes between $\{\bar{1}2\bar{1}0\}$ (planes perpendicular to the $<2\bar{1}\bar{1}0>$ direction, in blue) and $\{10\bar{1}0\}$ (planes perpendicular to the $<10\bar{1}0>$ direction, in green) are parallel to the surface of the coating. This result is consistent with XRD measurements, EBSD results obtained far from a whisker and with the study of Lindborg [9]. However, it is clearly shown that the crystallographic orientation of grains in the root region differs from this orientation as it is illustrated in Fig. 4 by grains with different colors. So, it must be mentioned that the difference of BC could, in this case, also be attributed to the difference of orientation between grains in the root region and in the columnar region. However, this observation

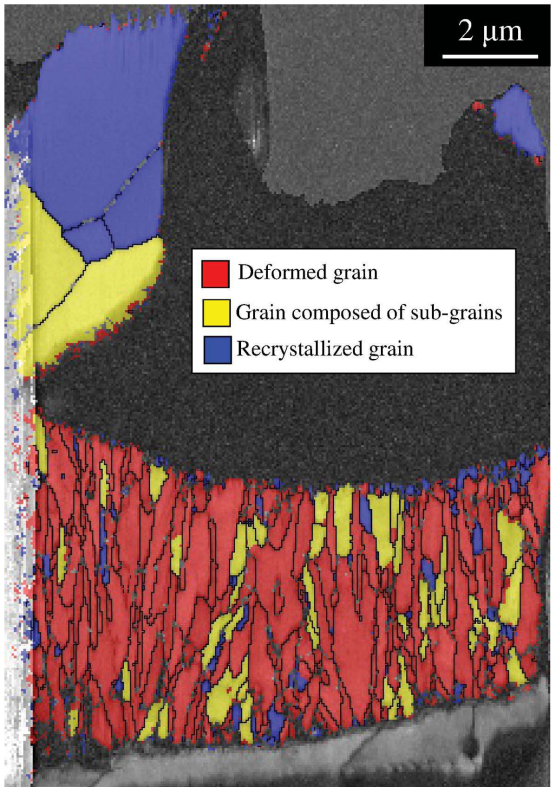

Fig. 5. Misorientation cartography of the Zn coating obtained on the sample extracted at the root of a whisker superimposed on the EBSD pattern quality map. "Deformed grains" are grains whose average misorientation angle is higher than 0.9° (red). Grains can be composed of sub-grains. The average misorientation angle within the sub-grains is under 0.9°, but the misorientation from sub-grain to sub-grain is higher than 0.9° (yellow). All the remaining grains are "recrystallized grains" (blue).

strengthens the hypothesis that grains at the root of the whisker are recrystallized because recrystallized grains do not have the same orientation than the matrix [18], [19].

Finally, the misorientation cartography depicted in Fig. 5 also supports the recrystallization mechanism. The average misorientation angle within each grain is calculated. If it is higher than the minimum angle $\theta_{\min}$ specified by the user (0.9° in this paper), the grain is defined as a "deformed grain." They appear red in Fig. 5. Some grains can be composed of sub-grains. If the average misorientation angle within each sub-grain is under $\theta_{\min}$ but the misorientation from sub-grain to sub-grain is higher than $\theta_{\min}$, these grains are called "grains composed of sub-grains" and they are yellow in Fig. 5. All the remaining grains are classified as "recrystallized grains" and are represented in blue in the Fig. 5. Within the columnar region (Fig. 5), 80% of the grains are considered as "deformed grains"; whereas 15% are "sub-grains" and only 5% are recrystallized. On the contrary, in the root region, 70% of the grains are classified as recrystallized and 30% are classified as "grains composed of sub-grains."

IV. Discussion

BC image, orientation maps and misorientation cartography obtained by EBSD suggest that grains at the root of the whisker are recrystallized. This conclusion is in agreement with tin whisker growth models based on recrystallization [19], [20]. In both models, the coating is composed by columnar grains under a compressive stress. First, Smetana [20] explains that some oblique grain boundaries can be formed during recrystallization of the coating. As the coating is under compressive stress, a force is applied on these oblique grain boundaries which can cause grain boundary sliding. This grain boundary sliding results in the formation of a whisker. A diffusion process, driven by a gradient of stress from vertical grain boundaries to oblique grain boundaries and to the whisker grain, enables atoms, required for the grain growth, to move from the coating to the base of the whisker. It must be noted that this model explains the stress relaxation of the system but not the driving force at the origin of the following whisker growth. As already experimentally observed in Sn coatings [20], [21] and predicted by the model, oblique grain boundaries are clearly visible at the root of the whisker. In the model, vertical grain boundaries play a key role in the diffusion process, however, no vertical grain boundaries are experimentally observed below oblique grain boundaries.

Vianco *et al.* [19] describe the whisker growth by a cyclic dynamic recrystallization (DRX) mechanism. Due to the compressive stress, dislocations are created and pile up at a vertical grain boundary. The storage of energy due to the piling up of dislocations results in the formation of a new grain free of defects at the vertical grain boundary. Once the new grain has reached its maximum size in the coating, it grows at the surface of the coating in form of a whisker. In this paper, it clearly appears that a grain growth occurs at the root of the whisker. According to Vianco *et al.*, one criterion for the cyclic DRX is that $D_0 < 2D_x$, where D_0 and D_x are, respectively, the initial grain size and the final grain size. This criterion is satisfied here as initial grains are 270 nm wide and 1.50 μm long and recrystallized grains are larger than 2 μm. It should, however, be noticed that some discrepancies appear between our experimental data and this last model predictions. First, it is clear from SEM images that several grains have been recrystallized while only one is predicted by the DRX model. Secondly, even though the whisker himself has not been analyzed by EBSD, there is no preferential orientation of the recrystallized grains as predicted by Vianco *et al.*, such as the {0001} planes parallel to the surface.

Results presented in this paper are a part of an experimental work performed on several zinc whiskers. It should be pointed out that Al, Ca, and C inclusion are not present under other whiskers but all other results, not presented here, indicate that recrystallized grains are located at the whisker root.

Owing to these new results and comparison to literature, a new whisker growing model is under consideration and will be reported in the future.

V. Conclusion

A sample for EDS and EBSD analysis was removed from the Zn coating of an electroplated steel prone to whiskering. Care was taken to be sure that it was prepared under a whisker, at the whisker root.

EDS analysis of the sample showed the presence of a C, Ca, and Al enriched inclusion. The impurities could have been

trapped during the electrodeposition or during a water rinsing. EBSD analysis highlights two distinct regions into the Zn coating.

1) The columnar region with columnar grains and vertical grain boundaries. Grains within this region are oriented with planes between $\{\bar{1}2\bar{1}0\}$ and $\{10\bar{1}0\}$ parallel to the surface of the coating. Most of the grains are classified as "deformed" grains. This grain structure is similar to the one into the Zn coating far from whiskers.
2) The root region with larger grains than in the columnar region. Grains exhibit oblique grain boundaries and do not have the same crystallographic orientation than grains in the columnar region. Grains in this region have a higher quality factor than grains in the columnar region and most of them are considered as recrystallized.

EBSD results showed that grains at the root of the whisker were recrystallized. This is in agreement with recent whisker growth models that involve recrystallization for whisker formation.

ACKNOWLEDGMENT

The authors would like to thank L. Chevalier at GPM, Rouen, France, for the energy-dispersive spectroscopy analyses.

REFERENCES

[1] H. L. Cobb, "Cadmium whiskers," *Monthly Rev. Am. Electroplat. Soc.*, vol. 33, no. 28, pp. 28–30, 1946.
[2] G. T. Galyon, "Annotated tin whisker bibliography and anthology," *IEEE Trans. Electron. Packag. Manuf.*, vol. 28, no. 1, pp. 94–122, Jan. 2005.
[3] G. T. Galyon and L. Palmer, "An integrated theory of whisker formation: The physical metallurgy of whisker formation and the role of internal stresses," *IEEE Trans. Electron. Packag. Manuf.*, vol. 28, no. 1, pp. 17–30, Jan. 2005.
[4] E. Chason, N. Jadhav, W. L. Chan, L. Reinbold, and K. S. Kumar, "Whisker formation in Sn and Pb-Sn coatings: Role of intermetallic growth, stress evolution, and plastic deformation processes," *Appl. Phys. Lett.*, vol. 92, no. 17, pp. 171901-1–171901-3, 2008.
[5] S. Lal and T. D. Moyer, "Role of intrinsic stresses in the phenomena of tin whiskers in electrical connectors," *IEEE Trans. Electron. Packag. Manuf.*, vol. 28, no. 1, pp. 63–74, Jan. 2005.
[6] H. G. Smith and R. E. Rundle, "X-ray investigation of perfection in tin whiskers," *J. Appl. Phys.*, vol. 29, no. 4, pp. 679–683, Apr. 1958.
[7] M. W. Barsoum, E. N. Hoffman, R. D. Doherty, S. Gupta, and A. Zavaliangos, "Driving force and mechanism for spontaneous metal whisker formation," *Phys. Rev. Lett.*, vol. 93, no. 20, pp. 206104-1–206104-4, 2004.
[8] J. Brusse and M. Sampson, "Zinc whiskers: Hidden cause of equipment failure," *IEEE Comput. Soc.*, vol. 6, no. 6, pp. 43–47, Nov.–Dec. 2004.
[9] U. Lindborg, S. Ramsin, L. Lind, and L. Révay, "Microstructure and Metallurgical properties of some zinc electroplates," *Plating*, vol. 61, pp. 1111–1116, 1974.
[10] A. Baated, K.-S. Kim, and K. Suganuma, "Whisker growth from an electroplated zinc coating," *J. Mater. Res.*, vol. 25, no. 11, pp. 2175–2182, 2010.
[11] H. L. Reynolds and R. Hilty, "Investigations of zinc (Zn) whiskers using FIB technology," in *Proc. IPC/JEDEC Lead Free North Amer. Conf.*, Boston, MA, 2004, pp. 1–7.
[12] A. Lina and M. Mahe, "Essai en enceinte climatique pour l'étude de la formation et de la croissance des whiskers de zinc et de cadmium," EDF, Moret sur Loing Cedex, France, Tech. Rep. H-T29-2009-04050-FR, 2009.
[13] G. Permigiani, "Wässeriges, saures bad für zinkplattierungsverfahren und das bad verwendes zinkplattierungsverfahren," E.P. Patent 1 070 771, Jan. 24, 2001.
[14] B. Schmitz and M. Larnicol, "Influence de paramétres process sur la chimie de surface des aciers galvanisés et impact sur leur réactivité vis à vis des traitements de conversion," *GIS Surf. J. Thématiques Résist. Corros.*, Jun. 2008.
[15] T. Maitland and S. Sitzman, *Scanning Microscopy for Nanotechnology Techniques and Applications*, W. Zhou and Z. L. Wang, Eds. New York: Springer-Verlag, 2007, pp. 41–75.
[16] M. Kamay, A. J. Wilkinson, and J. M. Titchmarsh, "Measurement of plastic strain of polycrystalline material by electron backscatter diffraction," *Nucl. Eng. Design*, vol. 235, no. 6, pp. 713–725, 2005.
[17] A. J. Wilkinson and D. J. Dingley, "Quantitative deformation studies using electron back scatter patterns," *Acta Metall. Mater.*, vol. 39, no. 12, pp. 3047–3055, 1991.
[18] M. Colombié, *Matériaux Métalliques*, 2nd ed. Paris, France: L'Usine Nouvelle, 2008.
[19] P. T. Vianco and J. A. Rejent, "Dynamic recrystallization (DRX) as the mechanism for Sn whisker development. Part I: A model," *J. Electron. Mater.*, vol. 38, no. 9, pp. 1815–1825, 2009.
[20] J. Smetana, "Theory of tin whisker growth: The end game," *IEEE Trans. Electron. Packag. Manuf.*, vol. 30, no. 1, pp. 11–22, Jan. 2007.
[21] C. Xu, Y. Zhang, C. Fan, J. Abys, L. Hopkins, and F. Stevie, "Understanding whisker phenomenon: Driving forces for the whisker formation," in *Proc. IPC SMEMA APEX Conf.*, 2002, pp. S06-2-1–S06-2-6.